Proceedings of IPACK2007
ASME InterPACK '07
July 8-12, 2007, Vancouver, British Columbia, CANADA

IPACK2007-33246

A MATHEMATICAL MODEL PREDICTING HEAT TRANSFER PERFORMANCE IN A OSCILLATING HEAT PIPE

H. B. Ma, B. Borgmeyer, P. Cheng, and Y. Zhang

Department of Mechanical & Aerospace Engineering
University of Missouri-Columbia
Columbia, MO 65211

ABSTRACT

A mathematical model predicting the oscillating motion in an oscillating heat pipe is developed. The model considers the vapor bubble as the gas spring for the oscillating motions including effects of operating temperature, non-linear vapor bulk modulus, and temperature difference between the evaporator and the condenser. Combining the oscillating motion predicted by the model, a mathematical model predicting the temperature drop between the evaporator and the condenser is developed including the effects of the forced convection heat transfer due to the oscillating motion, the confined evaporating heat transfer in the evaporating section, and the thin film condensation in the condensing section. In order to verify the mathematical model, an experimental investigation was conducted. Experimental results indicate that there exists an onset power input for the excitation of oscillating motions in an oscillating heat pipe, i.e., when the input power or the temperature difference from the evaporating section to the condensing section was higher than this onset value the oscillating motion started, resulting in an enhancement of the heat transfer in the pulsating heat pipe. Results of the investigation will assist in optimizing the heat transfer performance and provide a better understanding of heat transfer mechanisms occurring in the oscillating heat pipe.

INTRODUCTION

Because of the rapid development of the electronic industry, with chips packed closer together and the continuing decrease in the size of electronic packages, heat flux levels continue to increase. For example, the new design of high-density computer chips for the next generation of desktop computers may reach a heat flux level of over 80 W/cm^2. Metal oxide semiconductor controlled thyristors generate heat fluxes from 100 to 200 W/cm^2. And some laser diode applications have reached a heat flux level of 500 W/cm^2. Conventional heat sinks or spreaders become severely inadequate at these high levels of heat fluxes. While the conventional heat pipe can significantly push the border of cooling power, the heat transfer limitations in the heat pipe restrict the applications for these high levels of heat fluxes.

Compared with the conventional heat pipe, the successful oscillating heat pipe (OHP) has the following features: 1) because most or all of working fluid does not flow through the wick structure, there is a low pressure drop of working fluid; 2) because the vapor flow direction is the same as liquid flow, there is no vapor flow influence on the liquid flow; 3) the thermally driven, oscillating flow inside the capillary tube will effectively produce some "blank" surfaces to significantly enhance evaporating and condensing heat transfer; and 4) due to the oscillating motion in the capillary tube, the heat added on the evaporating area can be distributed by the forced convection in addition to the phase-change heat transfer. Clearly, the OHP exists a potential to remove an extra high level of heat flux.

Extensive experimental investigations [1-6] and theoretical analysis [7-15] have been conducted, and show that there exist oscillating or/and oscillating motions in an oscillating heat pipe, which depend on working fluids [2-4], tilt angles [5-7], dimensions [2,6,9,10,13], filled liquid ratio [5,9,14], turns [2,4,13] and heat flux levels [2,4,7,14]. While these investigations have provided an insight into the mechanisms of oscillating motions occurring in the OHP, the primary factors affecting the heat transport capability have not been fully understood. As mentioned above, the OHP transfers heat through forced convection in addition to phase-change heat transfer. It is expected that the heat transport capability occurring in the OHP should be much higher than the convectional heat pipe. But, the available experimental data show that the effective thermal conductivity occurring in the OHP is lower. In this investigation, a mathematical model predicting the temperature drop from the evaporating section to the condensing section is developed to determine the primary

factors affecting the heat transport capability in the OHP, which includes the oscillating motion occurring in the OHP, confined convection boiling, and film condensation. In order to verify the model presented in the paper, an experimental investigation was conducted.

NOMENCLATURE

A	cross sectional area of tube, m^2
c	specific heat of fluid, J/kg.K
G	mass flux, , kg/m^2
h	heat transfer coefficient, W/m^2K
h_{fg}	latent heat, kJ/kg
k	thermal conductivity of fluid, W/m.K
L	length of fluid, m
$m_{v,e}$	vapor produced in evaporator, $kg/(sm^2)$
$m_{l,c}$	liquid condensed in condenser, $kg/(sm^2)$
p	pressure, N/m^2
q''	heat flux, W/m^2
T	temperature, K
u_a	average oscillation velocity in z direction, m/s
D	tube diameter, m
x	quality
z	direction, m

Greek Symbols

ϕ	filled liquid ratio
ρ	density, kg/m^3
μ	viscosity, $N.s/m^2$
ζ	damping ratio
τ	time, s

Subscripts

e	evaporator
c	condenser
i	inside
l	liquid
v	vapor
w	wall

THEORETICAL ANALYSIS

To simplify the problem and find the primary factors affecting the heat transfer performance in an OHP, consider an oscillating heat pipe as shown in Fig. 1, which consists of an evaporating section, an adiabatic section, and a condensing section. As heat is added on the evaporating region in the OHP, the liquid is vaporized, causing the vapor volume expansion. Vapor in the condensing region is condensed into liquid, causing the volume contraction. The volume expansion and contraction excites an oscillation motion of the liquid plugs and vapor bubbles in the channels. Through the forced convection and phase-change heat transfer, heat is transferred from the evaporating section to the condensing section. Clearly, heat transfer in the OHP involves the evaporating heat transfer in the evaporating section, condensing heat transfer in the condensing section, and oscillating motions in the whole heat pipe.

Heat Transfer in the Evaporating Section

When applying a heat source to the external circumference of the evaporator section, as shown in Fig. 1, heat is transported by conduction through the evaporator wall and reaches the working fluid, resulting in vaporization. The vapor volume expansion in the evaporating section combined with the vapor volume contraction in the condensing section generates the forced convection in the OHP. If the tube structuring the evaporating section is smooth, i.e., no wick structures on the inside surface of tube, the heat transfer process occurring in the evaporating section is similar to convection boiling heat transfer, which has been extensively investigated [16-23]. The heat transfer in the evaporating section of the OHP is similar to the boiling convection of two-phase flow through a tube, which can be described by both the nucleate boiling (microscopic) and bulk convection (macroscopic). The total heat transfer coefficient, h, can be expressed as

$$h = h_{mic} + h_{mac} \tag{1}$$

where h_{mic} is due to the nucleate boiling heat transfer, and h_{mac} due to the bulk convection caused by oscillating motions. Chen [16] developed a model describing the nucleate boiling heat transfer, where the microscopic nucleate boiling portion of the heat transfer coefficient could be found by

$$h_{mic} = 0.00122\left[\frac{k_l^{0.79} c_{pl}^{0.45} \rho_l^{0.49}}{\sigma^{0.5} \mu_l^{0.29} h_{lv}^{0.24} \rho_v^{0.24}}\right]\left[T_w - T_{sat}(P_l)\right]^{0.24}\left[P_{sat}(T_w) - P_l\right]^{0.75} S \tag{2}$$

where S is a suppression factor and a function of the two-phase Reynolds number, i.e.,

$$S = (1 + 2.56\times10^{-6}\,\mathrm{Re}_{tp}^{1.17})^{-1} \tag{3}$$

The two-phase Reynolds number in Eq. (3) can be determined by

$$\mathrm{Re}_{tp} = \mathrm{Re}_l [F(X_{tt})]^{1.25} \tag{4}$$

where the liquid Reynolds number and the Martinelli parameter, X_{tt}, are defined by

$$\mathrm{Re}_l = \frac{G(1-x)D_i}{\mu_l} \tag{5}$$

$$X_{tt} = \left(\frac{1-x}{x}\right)^{0.9}\left(\frac{\rho_v}{\rho_l}\right)^{0.5}\left(\frac{\mu_l}{\mu_v}\right)^{0.1} \tag{6}$$

respectively. The function $F(X_{tt})$ shown in Eq. (4) depends on the Martinelli parameter, i.e.,

$$F(X_{tt}) = 1 \quad \text{for} \quad X_{tt}^{-1} \le 0.1 \tag{7}$$

$$F(X_{tt}) = 2.35(0.213 + \frac{1}{X_{tt}})^{0.736} \quad \text{for} \quad X_{tt}^{-1} > 0.1 \tag{8}$$

With a given liquid filled ratio, ϕ, the quality, x, shown in Eq. (6), can be determined by

$$x = \frac{\rho_v - \phi\rho_v}{\overline{\rho}} \tag{9}$$

where the average density of working fluid in the system may be calculated by the following relation of

$$\frac{1}{\overline{\rho}} = \frac{x}{\rho_v} + \frac{1-x}{\rho_l} \tag{10}$$

Utilizing the Martinelli parameter for a two-phase flow, the heat transfer coefficient due to the forced convection caused by oscillating motions can be readily determined by

$$h_{mac} = F\left(X_{tt}\right) h_l \tag{11}$$

where h_l is the liquid-phase heat transfer coefficient defined as

$$h_l = 0.023\left(\frac{k_l}{D_i}\right) \mathrm{Re}_l^{0.8}\, \mathrm{Pr}_l^{0.4} \tag{12}$$

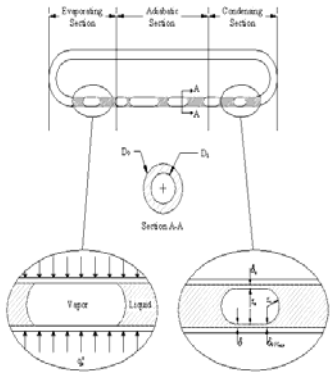

Fig. 1 Schematic of an oscillating heat pipe

Oscillating Motions

Examining the oscillating phenomena occurring in an OHP, there exist four kinds of forces, i.e., the thermally driven force, the capillary force, the frictional force, and the elastic restoring force. Based on the Newton's Laws, $\sum F = md^2x/d\tau^2$, Ma et al. [14] established a mathematical model describing the motion of the working fluid in an OHP as

$$\begin{aligned}&\left(L_l\rho_l + L_v\rho_v\right)A\frac{d^2x}{d\tau^2} + \left[\left(f_l\cdot \mathrm{Re}_l\right)\left(\frac{\mu_l L_l}{2D_h^2}\right) + \left(f_v\cdot \mathrm{Re}_v\right)\left(\frac{\mu_v L_v}{2D_h^2}\right)\right] \\ &\cdot A\frac{dx}{d\tau} + \frac{A\rho_v RT}{L_v}x = \left(\frac{Ah_{fg}\rho_{v,c}}{T_e}\right)\left(\frac{\Delta T_{\max} - \Delta T_{\min}}{2}\right)[1+\cos(\omega\tau)]\end{aligned} \tag{13}$$

Utilizing Laplace transforms, the exact solution can be readily obtained,

$$x(\tau) = \frac{B}{m}\left[\frac{\left(\sqrt{\zeta^2-1}\right)\sin(\omega\tau) - e^{-\zeta\omega\tau}\sinh\left[\omega\left(\sqrt{\zeta^2-1}\right)\tau\right]}{2\zeta\omega^2\sqrt{\zeta^2-1}} + \frac{1 - e^{-\zeta\omega\tau}\left[\cosh\left(\left(\sqrt{\zeta^2-1}\right)\omega\tau\right) + \frac{\zeta\sinh\left(\left(\sqrt{\zeta^2-1}\right)\omega\tau\right)}{\sqrt{\zeta^2-1}}\right]}{\omega^2}\right] \tag{14}$$

where

$$m = A\left(\rho_L L_L + \rho_V L_V\right) \tag{15}$$

$$c = A\left[\left(f_l\cdot \mathrm{Re}_l\right)\left(\frac{\mu_l L_l}{2D_h^2}\right) + \left(f_v\cdot \mathrm{Re}_v\right)\left(\frac{\mu_v L_v}{2D_h^2}\right)\right] \tag{16}$$

$$k = \frac{A\rho_V RT}{L_V} \tag{17}$$

$$B = \left(\frac{Ah_{fg}\rho_{v,c}}{T_e}\right)\left(\frac{\Delta T_{\max} - \Delta T_{\min}}{2}\right) \tag{18}$$

For the system described by Eq. (14), the undamped natural frequency, ω_0, and a damping ratio, ζ, can be written as,

$$\omega_0 = \sqrt{\frac{k}{m}} \tag{19}$$

$$\zeta = \frac{c}{2m\omega_0} \tag{20}$$

respectively. The model considers the thermal energy from the temperature difference between the evaporator and condenser as the driving force for the oscillating motion. For a given temperature difference between the evaporator and condenser, the average velocity of oscillating motions occurring in the system can be readily calculated.

During the derivation of Eq. (13), it was assumed that x is small relative to Lv, the pressure variation at the time interval of $\Delta\tau$ in the vapor phase between the evaporator and condenser was based on

$$\Delta p_v = \frac{\rho_v RT}{L_v}x \tag{21}$$

As shown in Eq. (21), the vapor pressure is linearly dependent on x. For a given vapor volume, if the length of total vapor bubble is much longer than x, the assumption of linear relation between Δp_v and x is reasonable. Experimental results show that when the heat flux is higher, the aptitude and frequency significantly increase. If the total volume occupied by vapor at the time τ is V_v, i.e., L_vA, and vapor is assumed as an ideal gas, the vapor pressure at the time τ can be found as:

$$p_{v,\tau} = \frac{m_v RT}{L_v A} \tag{22}$$

At the time $\tau+\Delta\tau$, after heat is added to the evaporating section and evaporation occurs, the increase in the pressure will result in a decrease in the vapor volume by $-xA$, and the pressure in the vapor space yields:

$$p_{v,\tau+\Delta\tau} = \frac{m_v RT}{(L_v - x)A} \tag{23}$$

The pressure variation at the time interval of $\Delta\tau$ can be approximately written as:

$$\Delta p_v = \frac{\rho_v RT}{L_v}\left(x + \frac{x^2}{L_v} + \frac{x^3}{L_v^2} + \ldots + \frac{x^n}{L_v^{n-1}}\right) \tag{24}$$

Considering Eq. (24), Eq. (13) becomes:

$$\left[(f_l \mathrm{Re}_l)\left(\frac{\mu_l L_l}{2D_h^2}\right) + (f_v \mathrm{Re}_v)\left(\frac{\mu_v L_v}{2D_h^2}\right)\right] A\frac{dx}{d\tau} + \frac{A\rho_v RT}{L_v}\left(x + \frac{x^2}{L_v} + \frac{x^3}{L_v^2} + \ldots + \frac{x^n}{L_v^{n-1}}\right) \tag{25}$$
$$= \left(\frac{Ah_{fg}\rho_{v,c}}{T_e}\right)\left(\frac{\Delta T_{\max} - \Delta T_{\min}}{2}\right)\left[1 + \cos(\omega\tau)\right]$$

Heat Transfer in the Condensing Section

The vapor generated in the evaporating section is condensed in the condensing section if the phase-change driving force exists, and the condensate in the thin film region will flow into the liquid-slug region due to the capillary force. Because the film thickness in the condensing film region is very thin compared with the meniscus thickness in the liquid slug, most of the condensing heat transfer will occur in the thin film region as shown in Fig. 1. In this region, the Reynolds number of the condensate is very small, hence the inertial terms can be neglected and based on conservation of momentum in the thin film, the pressure drop due to the viscous flow can be found as

$$\frac{dP_l}{ds} = \frac{f \cdot \mathrm{Re}_\delta \, \mu_l D_o q_c'' s}{2\delta^3 D_i \rho_l h_{fg}} \tag{26}$$

where

$$\mathrm{Re}_\delta = \frac{\bar{U}_{l,c}\, \delta \rho_l}{\mu_l} \tag{27}$$

By integrating Eq. (26) from s=0 to $L_{c,v}/2$, the total pressure drop along half of the vapor bubble length can be found as:

$$\Delta P_l = \int_o^{\frac{L_{c,v}}{2}} \left(\frac{f \cdot \mathrm{Re}_\delta \, \mu_l D_o q_c''}{2\delta^3 D_i \rho_l h_{fg}}\right) s ds \tag{28}$$

There exist numerous vapor slugs in the OHP including the condensing section. Although the vapor slug distributions, i.e., vapor bubble number, in the OHP was unpredictable, the total vapor space was remained constant for a given liquid filled ratio, Φ, which is defined as:

$$\phi = \frac{V_l}{V} \tag{29}$$

where V_l is the volume occupied by liquid, and V is the total volume throughout the heat pipe. It is assumed that all of the vapor slugs in the condensing region are combined into one large slug with condensation occurring on its perimeter. Assuming a uniform distribution of vapor throughout the entire length of the heat pipe, the length of the idealized single vapor slug in the condenser may be found by:

$$L_{c,v} = L_c\left(1 - \phi\right) \tag{30}$$

The capillary pressure along the condensate film can be found as:

$$\frac{dP_c}{ds} = 2\sigma\frac{dK}{ds} \tag{31}$$

Integrating Eq. (31) from $K=1/r_o$ to $K=1/r_c$, the total capillary pressure can be found as:

$$\Delta P_c = \sigma\left(\frac{2}{r_c} - \frac{1}{r_o}\right) \tag{32}$$

where r_0 is the meniscus radius of the liquid-vapor interface at the line of symmetry, i.e., at s=0, and r_c is the meniscus radius of the liquid-vapor interface at the liquid slug, i.e., at $s=L_{c,v}$, which can be found by:

$$r_0 = \frac{1}{2}\left(D_i - 2\delta_0\right) \tag{33}$$

and

$$r_c = \frac{1}{2}\left(D_i - 2\delta_{0.5L_{c,v}}\right) \tag{34}$$

respectively. Considering Eqs. (33) and (34), the total capillary pressure can be rewritten as:

$$\Delta P_c = \sigma\left(\frac{2}{\left(\frac{D_i}{2} - \delta_{0.5L_{c,v}}\right)} - \frac{1}{\left(\frac{D_i}{2} - \delta_o\right)}\right) \tag{35}$$

For the steady-state condensation process of the thin film, the capillary pressure defined by Eq. (35) should be equal to the pressure drop determined by Eq. (28). With a given heat flux level, i.e., q_c'', Eqs. (35) and (28) can be readily solved and the condensation film thickness determined.

EXPERIMENTAL SYSTEM

In order to verify the analytical model predicting the heat transfer performance, experimental investigations were conducted. The experimental system, as shown in Fig. 2,

consisted of a test section including an oscillating heat pipe, a cooling bath, a power supply, and a data acquisition system. The oscillating heat pipe shown in Fig. 3 was made of copper tube. The inside and outside diameters of the tube were 1.65 mm and 3.175 mm, respectively. Aluminum cooling block connected to the cooling bath provided a constant temperature condenser. The evaporating section of the OHP was strip resistance heater that spanned the copper plate. The OHP was surrounded with fiberglass insulation to reduce the heat loss. Based on the insulation surface temperature, the calculated heat loss is less than 1.5 % of the total heat added on the OHP. Twelve thermocouples were used to measure the temperature distributions along the heat pipe. Multiple thermocouples were placed in the evaporator, adiabatic, and condenser regions to determine the temperature drop across the sections. The temperature data was directly sent to the National Instruments data acquisition system connected to a personal computer for data recording and analysis. The OHP was backfilled to a 50 % filling ratio with HPLC grade water.

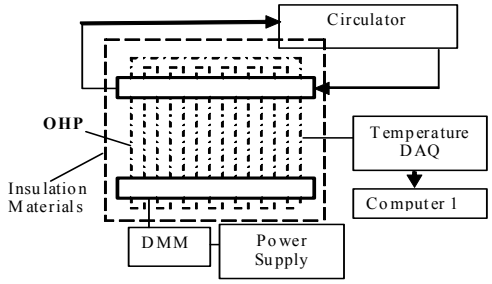

Fig. 2 Schematic of experimental system

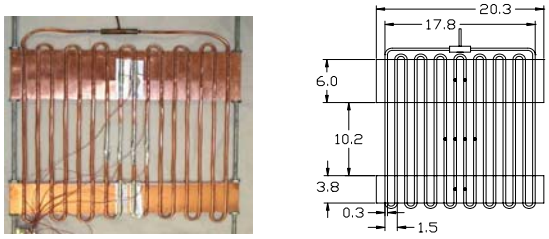

Fig. 3 Experimental heat pipe and dimensioned drawing (dimensions: cm)

Prior to the start of the experiment, the system was allowed to equilibrate and reach steady state such that the steady-state operating temperature was achieved and a uniform temperature distribution with no heater power input was observed throughout the OHP. Once the experimental system reached the steady state, the input power was increased in 50 W increments up to a maximum heat input of 350 W. The steady-state condition was defined as the mean temperature in the evaporator with a change of less than 0.5 °C in five minutes. To obtain the data for the next successive power level, the power was incremented approximately every 30 minutes. During the tests, the input power and temperature data, including the ambient temperature, were simultaneously recorded through the data acquisition system.

RESULTS AND DISCUSSION

The model for the fluid motion with the added non-linear terms has a different result from that originally presented by Ma et al. [14]. Figures 4 through 8 show the difference between the proposed non-linear model and the previously developed linear model for increasing operating temperatures. Figures 4, 5, 6, 7, and 8 displays the slug position with respect to time for operating temperature of 20 ^{o}C, 60 ^{o}C, 100 ^{o}C, 200 ^{o}C, and 300 ^{o}C, respectively. It can be seen that the new model slightly decreases the amplitude and frequency of the fluid motion. Also, as the operating temperature increases, the effect of the non-linear terms on the frequency is more prominent. Figure 9 shows the effect of increasing temperature drop on the fluid motion given the proposed model. It should be noted that increasing the temperature drop does not have an effect on frequency; however, the amplitude is greatly increased with a temperature drop increase.

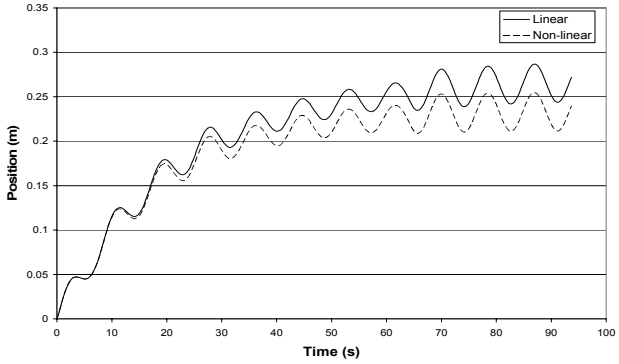

Fig. 4 Slug position versus time for linear and non-linear equations at an operating temperature of 20 ^{o}C.

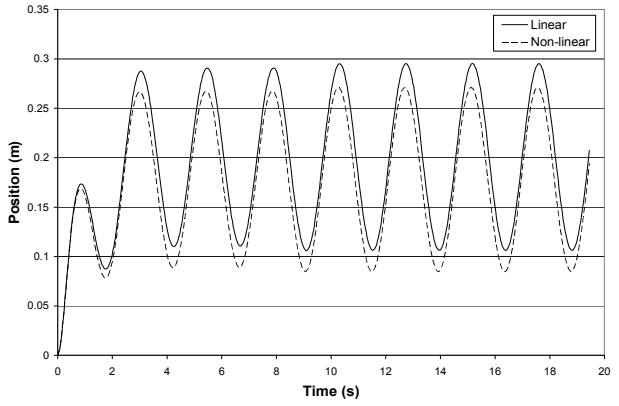

Fig. 5 Slug position versus time for linear and non-linear equations at an operating temperature of 60 ^{o}C.

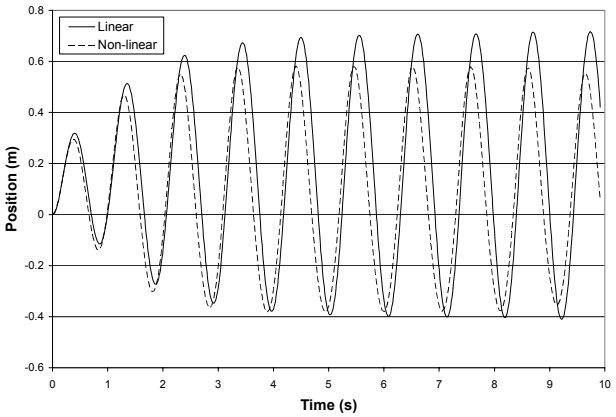

Fig. 6 Slug position versus time for linear and non-linear equations at an operating temperature of 100 ^{o}C.

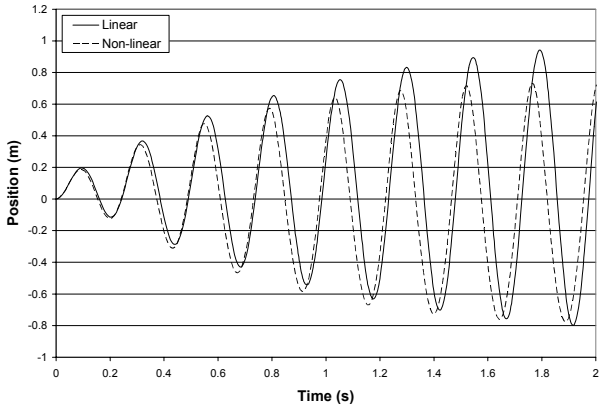

Fig. 7 Slug position versus time for linear and non-linear equations at an operating temperature of 200 ^{o}C.

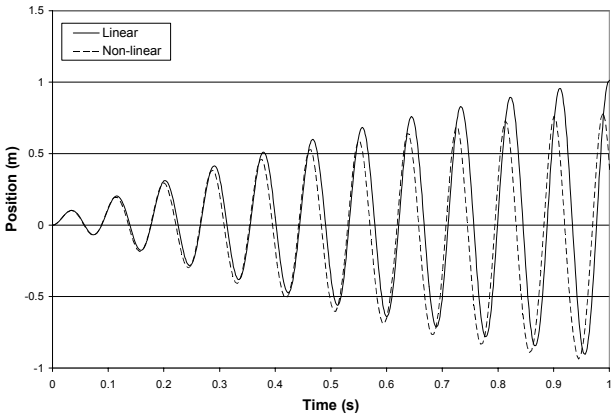

Fig. 8 Slug position versus time for linear and non-linear equations at an operating temperature of 300 ^{o}C.

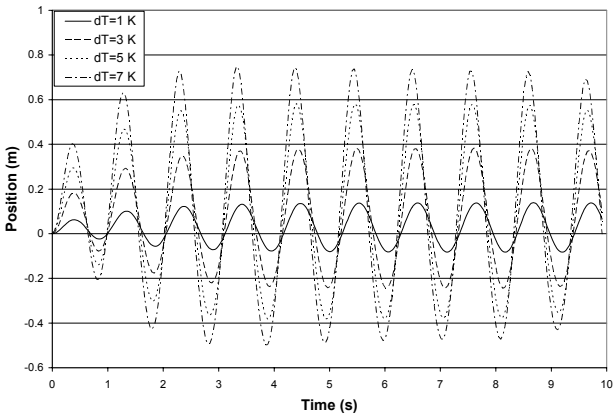

Fig. 9 Slug position versus time for non-linear equations at an operating temperature of 100 ^{o}C and varied temperature drop.

Figures 10 and 11 show the theoretical contribution of heat transfer in the micro and macro regions of the evaporator to the overall heat transfer coefficient for an operating temperature of 20 ^{o}C and 60 ^{o}C, respectively. As seen the contribution in the micro region, which is due to convective boiling, is much less than the heat transfer due to forced convection (i.e. macro region). Figure 12 and 13 display the theoretical evaporator, condenser, and total temperature drops in the specified OHP for an operating temperature of 20 ^{o}C and 60 ^{o}C, respectively. The temperature drop in the evaporator section contributes more to the total temperature drop than that in the condenser.

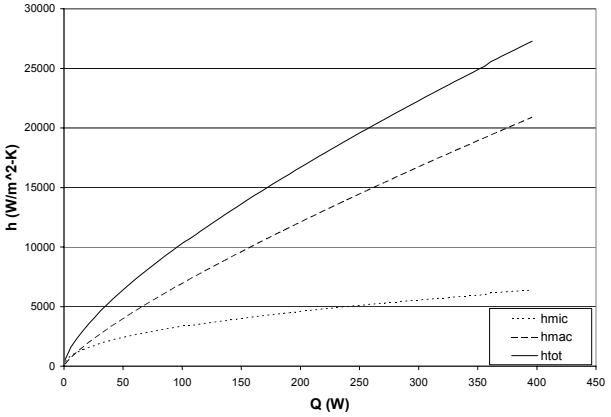

Fig. 10 Micro, macro, and total heat transfer coefficients versus heat input at an operating temperature of 20 ^{o}C.

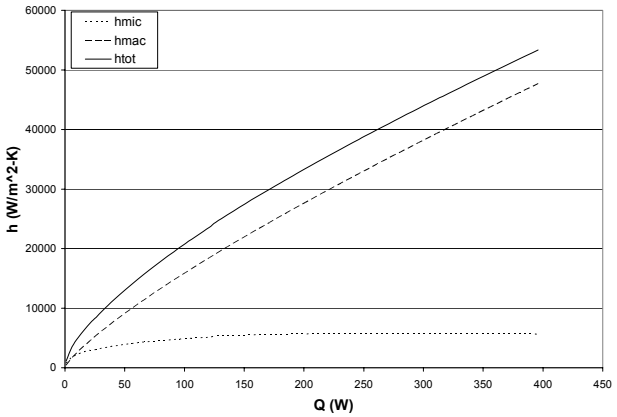

Fig. 11 Micro, macro, and total heat transfer coefficients versus heat input at an operating temperature of 60 ^{o}C.

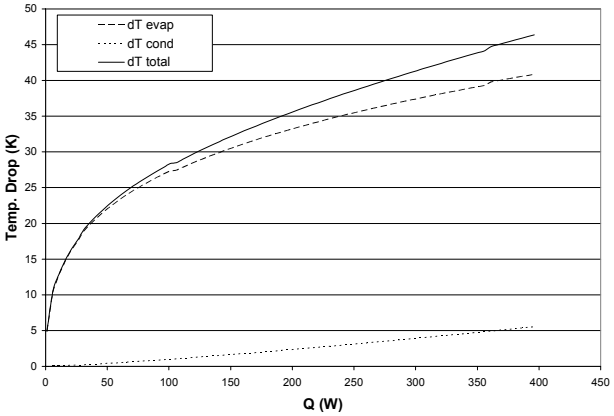

Fig. 12 Evaporator, condenser, and total temperature drop versus heat input at an operating temperature of 20 ^{o}C.

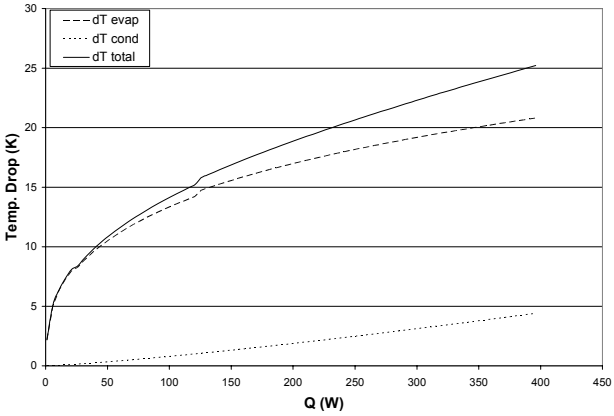

Fig. 13 Evaporator, condenser, and total temperature drop versus heat input at an operating temperature of 60 ^{o}C.

Experiments on the heat transfer performance of the OHP shown in Fig. 3 were performed and the results are presented in terms of the temperature drop from the evaporator to the condenser, ΔT_i, and heat input, Q. Temperature drops were based on the difference of the average recorded temperatures in the evaporator and condenser sections. Clearly, the oscillating motions generated in the heat pipe enhanced the heat transfer. When the input power was higher than 30 W, the oscillating motions started and the increase in temperature drop with respect to heat input was reduced. It can be concluded there exist an onset temperature difference for the start of oscillating motions and a range of temperature differences for the steady-state oscillating motion. Figure 14 shows the experimental results obtained from the specified OHP and compares the temperature drops determined with the theoretical model proposed herein. The figure shows the results for both an operating temperature of 20 ^{o}C and 60 ^{o}C. As shown in Fig. 14 , there is good agreement between the theoretical results and experimental data.

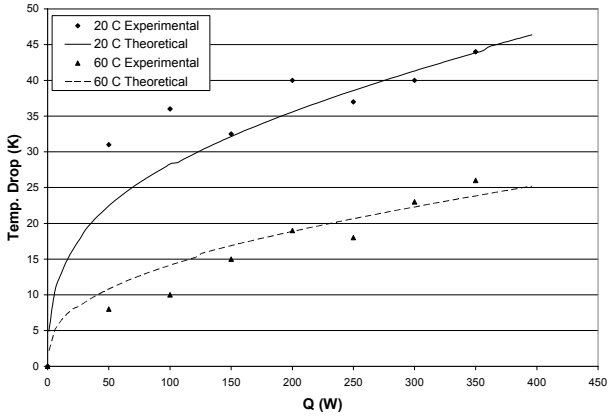

Fig. 14 Experimental and theoretical total temperature drops versus heat input at operating temperatures of 20 ^{o}C and 60 ^{o}C.

CONCLUSIONS

A mathematical model predicting the fluid motion and temperature drop in an oscillating heat pipe has been developed. The model includes the forced convection heat transfer due to the oscillating motions, the confined evaporating heat transfer in the evaporating section, and thin film condensation heat transfer in the condensing section. The numerical results indicate that the oscillating motions occurring in the oscillating heat pipe significantly enhances the heat transfer in the oscillating heat pipe. An experimental investigation of temperature drops occurring in an oscillating heat pipe was also conducted. Experimental results indicated that there exists an onset temperature difference for the excitation of oscillating motions in an oscillating heat pipe, i.e., when the input power or the temperature difference from the evaporating section to the condenser was higher than this onset value the oscillating motion started, resulting in an enhancement of the heat transfer. Results of the investigation will assist in optimizing the heat transfer performance and

provide a better understanding of heat transfer mechanisms occurring in the oscillating heat pipe.

REFERENCES

[1] Akachi, H., 1990, "Structure of a Heat Pipe," U.S. Patent #4,921,041.

[2] Ma, H.B., Wilson, C., Yu, Q, Choi, U.S., Tirumala, M., 2006 "An Experimental Investigation of Heat Transport Capability in a Nanofluid Oscillating Heat Pipe," ASME Journal of Heat Transfer, Vol. 128, November, pp.1213-1216.

[3] Zhang, X.M., Xu, J.L., Zhou Z.Q., 2004, "Experimental Study of a Pulsating Heat Pipe Using FC-72, Ethanol, and Water as Working Fluids," *Experimental Heat Transfer*, Vol. 17, pp. 47-67.

[4] Park, K. and Ma, H. B., 2007, "Nanofluid Efffect on the Heat Transfport Capability in a Well-Balanced Oscillating Heat Pipe," accepted for publication in AIAA Journal of Thermophysics and Heat Transfer.

[5] Kim, J. H., Lee, W. H., Jung, H. S., Kim, J. S., 2000, "Characteristics of Pressure Oscillation in Self-Excited Oscillating Heat Pipe Based on Experimental Study, " 6th International Heat Pipe Symposium, Chiang Mai, Thailand, pp. 263-272.

[6] Borgmeyer, B. and Ma, H.B., 2007, "Experimental Investigation of Oscillating Motions in a Flat Plate Pulsating Heat Pipe," accepted for publication in AIAA Journal of Thermophysics and Heat Transfer.

[7] Khandekar, S. and Groll, M., *An Insight into Thermo-Hydrodynamic Coupling in Closed Loop Heat Pipes*, Int. Journal of Thermal Sciences, 2003.

[8] Khandekar, S., Nanyam, S., and Groll, M., 2004, "Two-Phase Flow Modeling in Closed Loop Pulsating Heat Pipes," *13th International Heat Pipe Conference*, Sep. 19 – 25, 2004.

[9] Zuo, J., North M. T., and Wert K. L., 2001, "High Heat Flux Heat Pipe Mechanism for Cooling of Electronics," IEEE Transactions on Components and Packaging Technology, Vol. 24, No.2, pp.220-225.

[10] Liang, S. B., and Ma, H. B., 2003, "Oscillation Motions in an Oscillating Heat Pipe," *International Communication of Heat and Mass Transfer*,Vol. 43. No. 9, pp.493-500.

[11] Qu, W. and Ma, H.B., 2007, "Theoretical Analysis of Start-up of a Pulsating Heat Pipe," accepted for publication in the International Journal of Heat and Mass Transfer.

[12] Zhang, Y., and Faghri, A., 2003, "Oscillatory Flow in Pulsating Heat Pipes with Arbitrary Numbers of Turns, *Journal of Thermophysics and Heat Transfer*, pp. 340-347

[13] Zhang, Y. and Faghri, A., 2002, "Heat Transfer in an oscillating Heat Pipe with Open End, " International Journal of Heat and Mass Transfer, Vol. 45, No.4, pp. 755-764

[14] Ma, H. B., Hanlon, M.A., and Chen, C. L., 2006, "An Investigation of Oscillating Motions in a Miniature Pulsating Heat Pipe," *Microfluidics and Nanofluidics,* Vol. 2, No. 2, pp. 171-179.

[15] Wong T. N., Tong B. Y., Lim S. M. and Ooi K. T.,1999, "Theoretical Modeling of Oscillating Heat Pipe," Proceedings of 11th International Heat Pipe Conference, Tokyo, Japan, pp.159-163.

[16] Chen, J. C., 1966, "Correlation for Boiling Heat Transfer to Saturated Fluids in Convective Flow, Ind. Eng. Chem. Proc. Design and Dev., Vol., 5, No. 3, pp. 322-339.

[17] Zhao, T. S. and Cheng, P., 1998, "Heat Transfer in Oscillatory Flows," Annual Review of heat transfer, Volume IX, Edited by Tien, C. L.

[18] Wallis, G. B., 1969, One-dimensional two-phase flow, Mcgraw-Hill Book Company, New York

[19] Peterson, G. P., 1994, An Introduction to Heat Pipe: Modeling, Testing, and Applications, John Wiley & Sons, INC. New York

[20] Yuan, H., Oguz, H. N. and Prosperetti, A., 1999, "Growth and Collapse of a Vapor Bubble in a Small Tube," International Journal of Heat and Mass Transfer, Vol.42, Issue 19, pp. 3643-3657.

[21] Thomas, K. J. and Kim, C. J., 1998, "Valveless Pumping Using Traversing Vapor Bubbles in Microchannels," Journal of Applied Physics, Vol. 83, No. 11, pp. 5658-5664.

[22] Kurzweg, U. H., 1985, "Enhanced Heat Conduction in Fluids Subjected to Sinusoidal Oscillations," Journal of Heat Transfer, Vol. 107, No. 3, pp. 459-462.

[23] Kurzweg, U. H. and Zhao, L. D., 1984, "Heat Transfer by High-frequency Oscillations: A New Hydrodynamic Technique for Achieving Large Effective Thermal Conductivities," Phys. Fluids, Vol.27, No.11, pp. 2624-2627.